Felcman, J., Dolejší, V.

Adaptive Methods for the Solution of the Euler Equations in Elements of Blade Machines[a]

[a] ZAMM '95

The paper presents the use of an adaptive mesh refinement method devised for flow problems with shocks. The goal is to detect automatically the regions where the local structures such as shocks and contact discontinuities occur. During the computational algorithm these regions are refined with the aim to improve the quality of the previously computed approximation in a further computation. This can be accomplished with the aid of a suitable error indicator (for hyperbolic systems see e. g. [9, 11]) or by a shock indicator proposed in [5]. Here the numerical study of several shock indicators is presented.

1. Finite volume scheme

In a space-time cylinder $Q_T = \Omega \times (0,T)$ we consider the first order hyperbolic system

$$\frac{\partial w}{\partial t} + \sum_{s=1}^{2} \frac{\partial f_s(w)}{\partial x_s} = 0$$

describing inviscid compressible flow in a plane bounded domain Ω and time interval $(0,T)$. Here

$$w = (\rho,\, \rho v_1,\, \rho v_2,\, e)^{\mathrm{T}}, \quad w = w(x,t), \quad x \in \Omega, \quad t \in (0,T),$$

$$f_s(w) = (\rho v_s,\, \rho v_s v_1 + \delta_{s1} p,\, \rho v_s v_2 + \delta_{s2} p,\, (e+p)\, v_s)^{\mathrm{T}}$$

and p is given by the state equation

$$p = (\gamma - 1)\,(e - \rho |\boldsymbol{v}|^2/2).$$

We use the standard notation: t – time, x_s $(s = 1,2)$ – Cartesian coordinates, ρ – density, p – pressure, e – total energy, $\boldsymbol{v} = (v_1, v_2)$ – velocity, δ_{ij} – Kronecker delta, $\gamma > 1$ is the Poisson adiabatic constant.

The initial condition and a set of boundary conditions complete the above system. For their description see e. g. [1, 3, 4].

Let the domain Ω be approximated by a polygonal domain Ω_h. We construct a triangulation $\mathcal{T}_h$ of Ω_h with the usual properties (in the sense of the finite element method). Let us denote the number of triangles NELEM, the number of vertices NPOIN and the number of sides lying on the boundary Ω_h NBELM. Based on this triangulation we define a *finite volume* partition $\mathcal{D}_h = \{D_i\}_{i \in J}$ of the closure $\overline{\Omega}_h$ into a finite number of closed polygons D_i; J is a suitable index sets. Three types of finite volumes are considered, namely, triangular, dual and barycentric finite volumes as they are sketched in Figure 1.

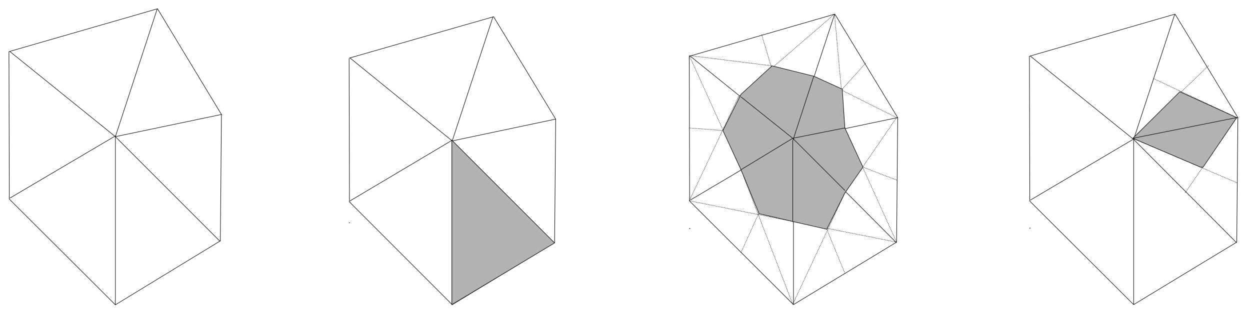

Triangular mesh | Triangular finite volume | Dual finite volume | Barycentric finite volume

Figure 1: Finite volume construction

As the triangular finite volumes the original triangles are considered. The dual finite volume D_i is defined as a box around any vertex P_i of the original triangulation. The boundary of the dual volume D_i consist of straight lines connecting for each triangle containing the vertex P_i its barycentre with the middle of the triangle side outgoing from P_i. The barycentric finite volume is a quadrilateral or a triangle. It is constructed in such a way that in each triangle the vertices are connected with the barycentre. The number of *triangular* finite volumes is NELEM. To each vertex of the triangulation a dual finite volume is assigned, so the number of *dual* finite volumes is NPOIN (in general, NELEM > NPOIN). The number of *barycentric* finite volumes is the same as is the number of sides in the triangulation, i. e. 3(NELEM/2) + NBELM/2 (which is evidently greater than NELEM).

We use a cell centred finite volume method, with constant values w_i^k representing the volume average of the vector of conserved quantities $w(\cdot, t_k)$ on D_i at time t_k. In each time step, the volume values are updated by approximating fluxes at the volume sides (see ([5])).

2. Refinement technique

The above defined three types of finite volumes can be given into the same context of the cell centred methods on finite volumes with arbitrary number of sides (faces in $3D$) and their combinations. There are two reasons that we do not do it and associate every finite volume mesh with the basic triangulation $\mathcal{T}_h$. First, the original triangulation is used for the conforming, as well as nonconforming finite element extension of finite volume method for an operator splitting solution of the complete Navier–Stokes system (see [2]). Second, the refinement procedure for the finite volume solution returns always to the original triangulation $\mathcal{T}_h$. This is straightforward for triangular finite volumes. For dual and barycentric finite volumes the piecewise constant approximate solution on finite volumes is converted to the piecewise constant function on the original triangular mesh. The weighted extrapolation technique is used. For any triangle $T_i \in \mathcal{T}_h$ we denote by $S(i)$ the set of indices j of neighbouring elements $T_j \in \mathcal{T}_h$ to T_i. By h_i we denote the length of the longest side of T_i. The shock is characterized by the jump up in the density and pressure and by the discontinuity of all state variables (see [8]). This is taken into account by the following shock indicators:

$$
\begin{aligned}
g_{\mathrm{rho}}(i) &= \max_{j \in S(i)} \left[-(\rho_i - \rho_j)\, \boldsymbol{v}_i \cdot \boldsymbol{n}_{ij}\right]^+ / h_i \\
g_v(i) &= \max_{j \in S(i)} \left[(|\boldsymbol{v}_i| - |\boldsymbol{v}_j|)\, \boldsymbol{v}_i \cdot \boldsymbol{n}_{ij}\right]^+ / h_i \\
g_p(i) &= \max_{j \in S(i)} \left[-(p_i - p_j)\, \boldsymbol{v}_i \cdot \boldsymbol{n}_{ij}\right]^+ / h_i \\
g_{\mathrm{group}}(i) &= \max_{j \in S(i)} \left\{\left[-(\rho_i - \rho_j)\, \boldsymbol{v}_i \cdot \boldsymbol{n}_{ij}\right]^+ + \left[(|\boldsymbol{v}_i| - |\boldsymbol{v}_j|)\, \boldsymbol{v}_i \cdot \boldsymbol{n}_{ij}\right]^+ \left[-(p_i - p_j)\, \boldsymbol{v}_i \cdot \boldsymbol{n}_{ij}\right]^+\right\} \Big/ h_i, \quad T_i \in \mathcal{T}_h.
\end{aligned}
$$

The superscript k is omitted because of simplicity, $\boldsymbol{n}_{ij}$ denotes the unit normal to the common side of T_i and T_j pointing out from T_i. The triangles with the value of the indicator greater then a prescribed tolerance are refined with the aid of the red-green refinement. For triangles with an angle greater than 110°, the red–green refinement is replaced by red*–green one according to Figure 2.

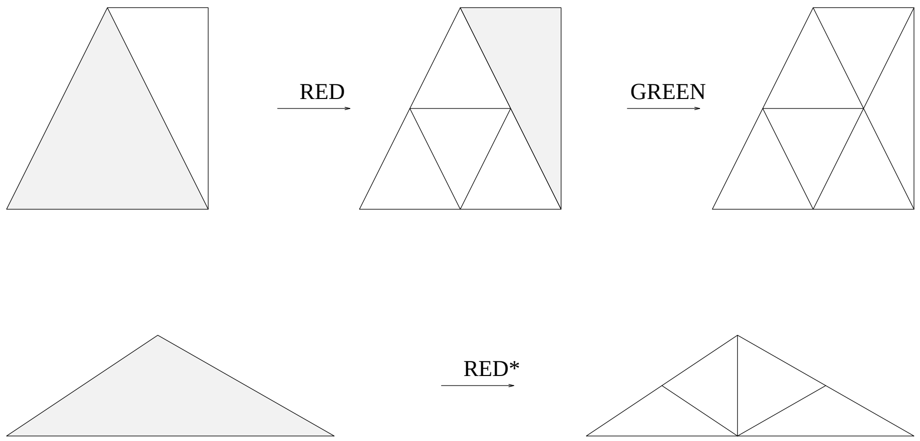

Figure 2: Refinement technique

This procedure can be applied to an arbitrary algorithm for the numerical prediction of flows with shocks if the approximate solution can be expressed by means of piecewise constant values on triangles.

3. Examples

In this section test cases are presented to demonstrate the performance of the proposed shock indicators. The comparison with the wind tunel experiment (see [10] and also [6]) justifies the g_{rho}-indicator as the best alternative. Figure 3 shows the basic mesh. Figures 4−6 represent the refinement based on the indicators g_v, g_p, g_{group}. In Figure 7 the refinement using g_{rho} is plotted. In Figure 8 the Mach number isolines computed on the refined mesh from Figure 7 are drawn. Another density based shock sensor is investigated in [7].

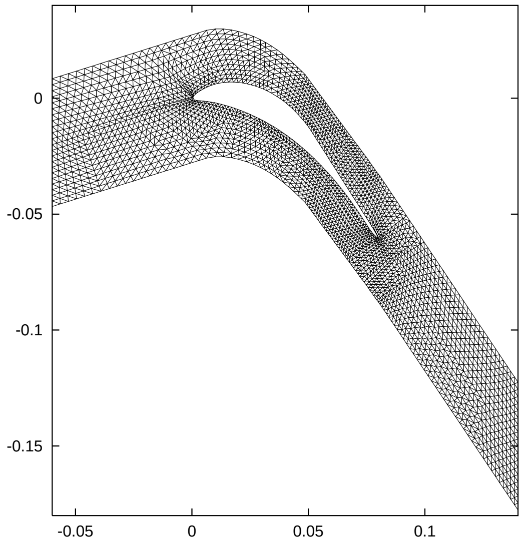

Figure 3: Basic mesh

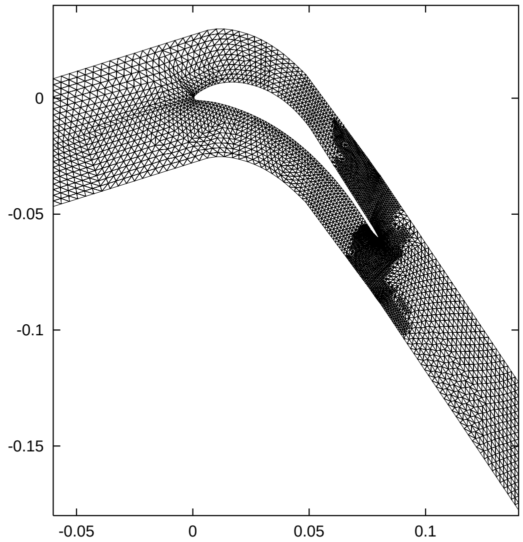

Figure 4: g_v-indicator refinement

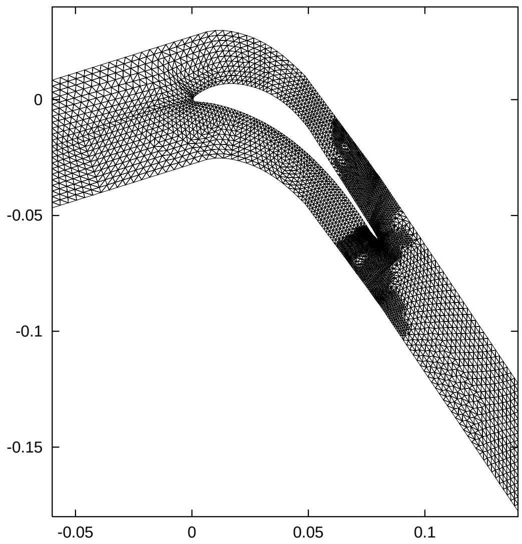

Figure 5: g_p-indicator refinement

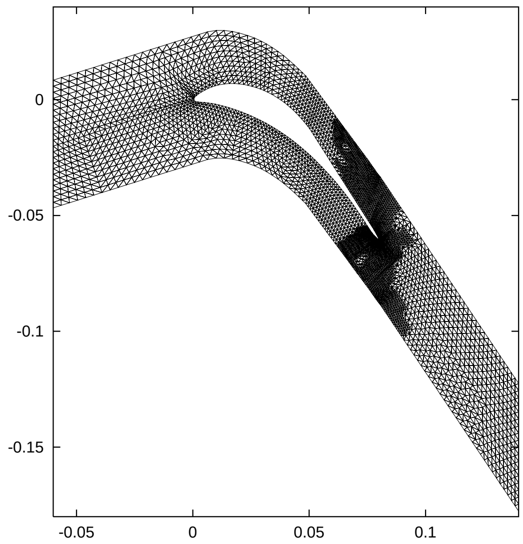

Figure 6: g_{group}-indicator refinement

Acknowledgements

This work was supported under the Grant No. 201/93/2177 of the Czech Grant Agency.

4. References

1 Feistauer, M.: Mathematical Methods in Fluid Dynamics; Pitman Monographs and Surveys in Pure and Applied Mathematics 67, Longman Scientific & Technical, Harlow, 1993, 457–460.

2 Feistauer, M., Felcman, J., Dolejší, V.: Numerical simulation of compressible viscous flow through cascades of profiles; ZAMM (this volume).

3 Feistauer, M., Felcman, J., Lukáčová–Medviďová, M.: Combined finite element – finite volume solution of compressible flow; J. Comput. Appl. Math. (to appear).

4 Felcman, J.: Application d'un schéma de Godunov à des écoulements transsoniques bidimensionnels; Actes de II èmes journées Saragosse – Pau de Mathématiques Appliquées, Université de Pau, 1995, 119–129.

5 Felcman, J., Dolejší, V., Feistauer, M.: Adaptive finite volume method for the numerical solution of the compressible Euler equations; Computational Fluid Dynamics 94 (Wagner, S., Hirschel, E. H., Périaux, J., Piva, R. – Eds.), Wiley, 1994, 894–901.

6 Fořt, J., Huněk, M., Kozel, K., Vavřincová, M.: Numerical simulation of steady and unsteady flows through plane cascades; Numerical Modelling in Continuum Mechanics II. (Feistauer, M., Rannacher, R., Kozel, K. – Eds.), Faculty of Mathematics and Physics, Charles University, Prague, 1995, 95–102.

7 Hentschel, R., Hirschel, E. H.: Self adaptive flow computations on structured grids; Computational Fluid Dynamics 94 (Wagner, S., Hirschel, E. H., Périaux, J., Piva, R. – Eds.), Wiley, 1994, 242–249.

8 Le Veque, R. J.: Numerical Methods for Conservation Laws; Birkhäuser Verlag, Basel – Boston – Berlin, 1990.

9 Sonar, T. H., Süli, A.: A dual graph-norm refinement indicator for finite volume approximations of the Euler equations; ICIAM 95, Hamburg, Book of abstracts, 1995, 178.

10 Šťastný, M., Šafařík, P.: Experimental analysis data on the transonic flow past a turbine cascade; ASME Publ. No. 90–GT–313, New York, 1990.

11 Warnecke, G.: Error estimates and adaptive methods for transonic flow problems; ICIAM 95, Hamburg, Book of abstracts, 1995, 123.

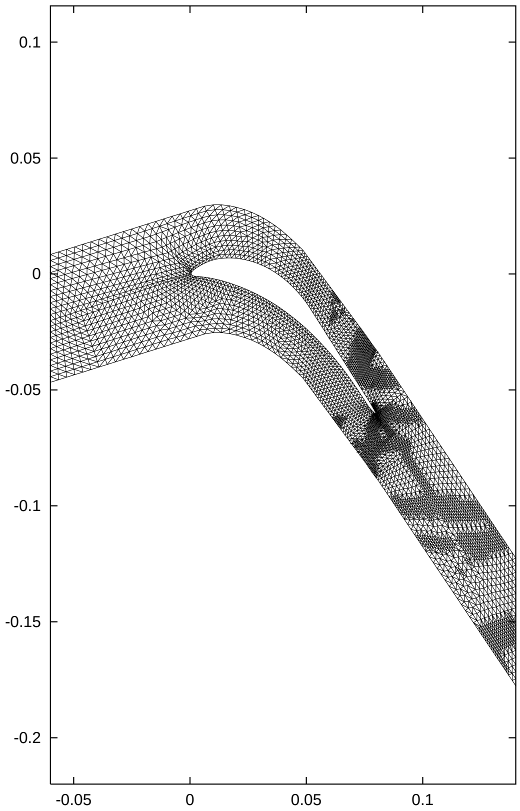

Figure 7: g_{rho}-indicator refinement

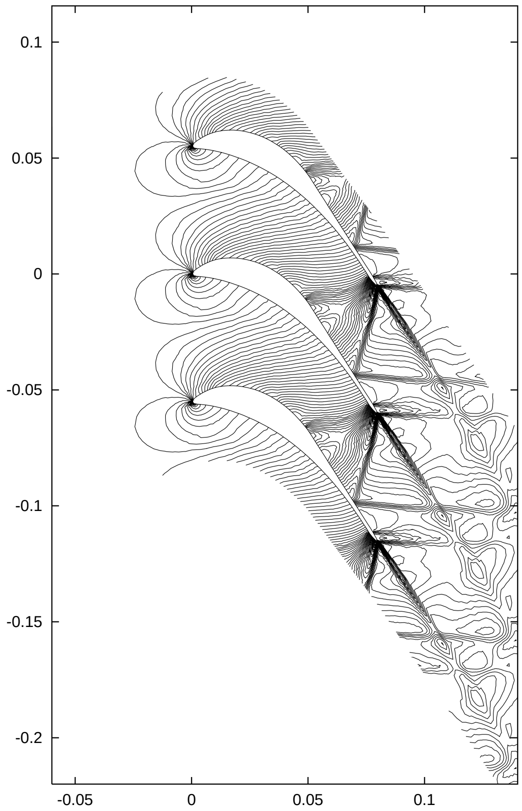

Figure 8: Mach number isolines

Addresses: Dr. Jiří Felcman, CSc., Vít Dolejší, Charles University, Faculty of Mathematics and Physics, Malostranské n. 25, 118 00 Praha 1, Czech Republic.